Available online at www.sciencedirect.com
ScienceDirect
Polymer 48 (2007) 502–511
polymer
www.elsevier.com/locate/polymer

Theoretical studies on the electronic structures and optical properties of the oligomers involving bipyridyl, thiophenyl and ethynyl groups

Tao Liu [a,b], Jin-Sheng Gao [b], Bao-Hui Xia [a,c], Xin Zhou [a], Hong-Xing Zhang [a,*]

[a] State Key Laboratory of Theoretical and Computational Chemistry, Institute of Theoretical Chemistry, Jilin University, Changchun 130023, PR China
[b] College of Chemistry, Heilongjiang University, Harbin 150080, PR China
[c] College of Chemistry, Jilin University, Changchun 130023, PR China

Received 4 July 2006; received in revised form 14 November 2006; accepted 14 November 2006
Available online 5 December 2006

Abstract

Structural, electronic, and optical properties of a series of π-conjugated chain type oligomers composed of the bipyridyl, ethynyl and thiophenyl fragments are studied by advanced quantum chemical methods. The properties of the P-oligomers (**P1**–**P4**, with 1–4 repeating units, respectively) and the corresponding DP-oligomers (**DP2**–**DP4**, with 2–4 repeating units, respectively, but without the terminal thiophenyl fragments) are compared. The geometry optimization results at B3LYP/6-31G level show that all the fragments involved in both the P-oligomers and DP-oligomers in the ground state exhibit a zigzag chain within the molecular plane. The TD-DFT calculations reveal that the dipole-allowed lowest-lying $X^1A \rightarrow A^1B$ absorption band of each oligomer possesses the $\pi \rightarrow \pi^*$ transition characters. The geometry structures of **P1**, **P2** and **DP2** in the excited state have been studied by the CIS method, the fluorescence of them revealed by TD-DFT method is originated from the $^1[\pi\pi^*]$ excited state. Upon increasing the number of the repeating unit, there is a progressive lowering in HOMO–LUMO gaps, being consistent with the red shifts in the lowest-lying absorptions and fluorescence. The ionization potentials (IPs) and electron affinities (EAs) of the polymer are obtained by the extrapolation method. The calculated IPs of DP-polymer are lower than those of P-polymer and the EAs of DP-polymer are higher than those of the P-polymer, which indicates that the DP-polymer is more suitable for electron transferring and hole creating material.

Keywords: Absorption; Fluorescence; Electronic structure

1. Introduction

In the past few decades, much attention has been paid to the study of the optical properties of the π-conjugated organic oligomer and polymer materials. Such great interests have been motivated by their extensive applications such as semiconducting devices [1], photovoltaic components [2], organic light-emitting diodes (OLEDs) [3], and field-effect transistors [4]. Indeed, the rich electrical and optical properties of these materials are originated from their special and tunable electronic structures. For example, the energy gap, which determines the optical properties of LEDs, can be regulated by the attached π-conjugated fragments. Therefore, the theoretical investigations on the geometry structures and the electronic structure of the materials in the ground and excited states are of practical significance. Ionization potentials (IPs), electron affinities (EAs), electron-extraction potentials (EEP) and hole-extraction potentials (HEP) indispensable of organic compounds are important parameters to evaluate the xerography, photography or electroluminescence properties. These parameters are valuable to access the abilities of the materials to transport and inject electrons and/or holes. In fact, these important electronic structural parameters can be obtained by means of theoretical calculation. On one hand, the theoretical calculation results can rationalize the properties of the materials, on the other hand, the calculation results provide

* Corresponding author. Fax: +86 431 8945942.
E-mail address: zhanghx@mail.jlu.edu.cn (H.-X. Zhang).

0032-3861/$ - see front matter © 2006 Elsevier Ltd. All rights reserved.
doi:10.1016/j.polymer.2006.11.029

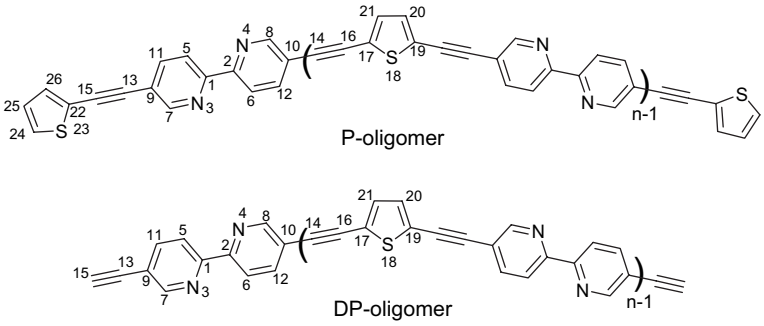

Fig. 1. Sketch structures of the P-oligomer and DP-oligomer.

guidance to experimental work. However, it is impossible to take the real polymer systems as the theoretical model object due to the limitation of the theory level and the vast size of the systems. This question was solved in 1987 by Lahti, who explored the extrapolation method [5] to investigate the excitation energy (E_g) of several potentially conducting conjugated polymers, in which a series of oligomers with different chain lengths were calculated, then the chain lengths were infinitely extrapolated to estimated the properties of the polymer. This approach is theoretically reliable since the conjugated oligomers have the characteristic to converge either in geometry structure or electronic structure as well as the spectroscopic properties.

So far, many π-conjugated oligomers have been studied and appear to be attractive luminescence materials [6–9]. In this family, most of the objects are P-type oligomers, where all the involved fragments are unsaturated groups. So far, a new type oligomers defined as DP-oligomers attract people's attention. In contrast to P-oligomers, the DP-oligomers are with a hydrogen atom to substitute the terminal unsaturated group in P-oligomers. Therefore, the electronic structures and the macroscopic properties of the DP-oligomers should have some change or be improved compared with the P-oligomers.

Recently a series of P-oligomers and corresponding DP-oligomers were synthesized by Ziessel and co-workers [10]. The oligomers are composed of the bipyridyl, thiophenyl, and ethynyl three groups (name as BTE) in each basic repeating unit. The defined P-oligomers are with the thiophenyl group as the end and the DP-oligomers terminate on ethynyl group. The UV–vis absorptions and fluorescence of these oligomers were investigated and showed a red-shift with the increase of the repeating units, but neither the electronic structures of the oligomers nor the properties of the polymer were reported.

Herein, we report the theoretical work on the oligomers containing the BTE units. We selected the theoretical models with 1–4 repeating units which are marked as **P1** (P-monomer), **P2** (P-dimer), **P3** (P-trimer) and **P4** (P-tetramer), and corresponding **DP2** (DP-dimer), **DP3** (DP-trimer) and **DP4** (DP-tetramer). A sketch of the chemical structure of the oligomers is depicted in Fig. 1. This work explored the geometry structures, electronic structures and the optical properties of the oligomers theoretically, aiming at providing an in-depth understanding on the correlation of the electronic structures with the properties. Through the comparison between the P-oligomers and DP-oligomers, the unusual and favorable properties of the DP-oligomers are revealed. Furthermore, the structures and the properties of the polymer are probed, which is of practical importance.

2. Computational details and theory

In the calculation, C_2 symmetry is adopted to settle the conformations of all the models both in the ground and in the excited states. As shown in Fig. 2, all of the oligomers are with the planar structure and display as the zigzag arrangement in the plane with the increase of the BTE units. To save the computation resources, we use the hydrogen atoms to replace the dibutyl group on the thiophenyl fragments appearing in the

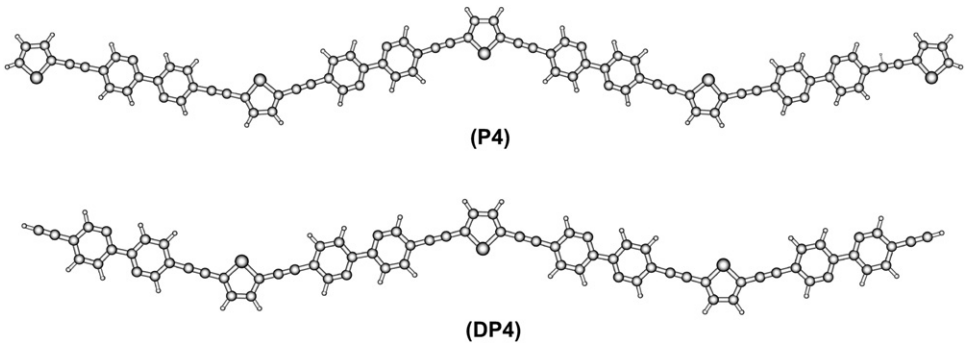

Fig. 2. The optimized geometry structures of **P4** and **DP4** in ground state at B3LYP level.

real molecules [10] since the dibutyl substituent can improve the solubility of the oligomers but hardly influence the spectral properties [10b]. In addition, the calculated low-lying absorption of **P1** just deviates 0.09 eV from that of the real monomer with dibutyl substituent on thiophenyl fragments. Therefore, the replacement of dibutyl with hydrogen doesn't change the intrinsic nature of the transition characters. Indeed, it is a general technique to employ the hydrogen atom to replace the methyl, phenyl, butyl, etc. in the calculation [11–13] for the simplification.

In our calculation, IPs, EAs, EEP and HEP are the differences of the energies between the ionic and the neutral molecules. The vertical IPs and EAs (labeled as *v*) are calculated with the optimized geometry of the neutral molecule while the corresponding adiabatic data (labeled as *a*) are obtained with the optimized geometry of the neutral and ionic molecules, respectively, the HEP and EEP are based on the geometry of the optimized cation and anion molecules, respectively. Energy gaps of the oligomers are always estimated by the energy difference between the highest occupied molecular orbital (HOMO) and the lowest unoccupied molecular orbital (LUMO). In this work, we also employ the extrapolation approach to acquire certain property of the polymer. Conventionally, the extrapolation approach adopted a linear-fitting scheme [5,6b]. However, we found that the present systems are more suitable for the binomial mode defined as $Y = a + bX + cX^2$, where X is equal to $1/n$ and is the reciprocal of the repeating unit numbers n, and Y is the value of certain property. As shown in infra parts, the binomial mode can offer the more precise extrapolation value in contrast to that of the monomial mode. All parameters correlative to the electronic structures such as IPs (*a*, *v*), EAs (*a*, *v*), HOMO–LUMO (H–L) gap, E_g, etc., and the optical properties of the polymers are obtained through the extrapolation project.

Previously, people studied the optical properties of π-conjugated oligomers with semiempirical methods such as AM1 and ZINDO approaches since these methods are not expensive [6] and can be performed on the large molecular systems, but the exact quantitative estimation of the electronic properties can hardly be extracted due to not only the insufficient description of the electron correlation effects but also the use of empirical parameters. In recent years, density functional theory (DFT) method has attracted a lot of attention because this method well considers the electronic correlation and can be applied to the large systems. Recent studies by Orti and Navarrete show that B3LYP (Becke's three parameter functional and the Lee–Yang–Parr functional) scheme is remarkably successful in resolving a wide variety of polymer systems [14], and it can yield the similar and reliable geometries for medium sized molecules as MP2 calculations did [15,16].

Configuration interaction singles (CIS) [17,18] method, presenting a general zeroth-order treatment to excited state just as HF for the ground state of molecular systems, is successful in the structure optimization of the excited state proved by many researchers [6,19]. The wave function, energy, and analytic gradient of a molecule in an electronic excited state are available for the CIS method [18,20,21]. However, the transition energies obtained by the CIS calculations are usually overestimated since the CIS method uses the orbitals of a HF state in an ordinary CI procedure to solve the higher roots and only considered parts of the electronic correlation effects via the mixing of excited determinants [20,21]. In our work, we rectify the excited state properties by time-dependent DFT (TD-DFT) method to compensate the flaw of the CIS method.

The geometry structures of **P1**–**P4** and **DP2**–**DP4** in the ground and excited states were fully optimized at the B3LYP and CIS level, respectively, with the 6-31G basis set for H, C and N atoms and 6-31G* basis set with one d-polarization function for S atom. Because the calculation to the excited state requires significantly more computational resource than that to the ground state, so we only studied the properties of **P1**, **P2** and **DP2** in the excited state as the prototype. IPs, EAs, HEP, EEP and H–L gap are calculated by DFT method. The absorptions and fluorescence are calculated by TD-DFT approach on the optimized geometry structures in the ground and excited states, respectively. All of the calculations are carried out with Gaussian 03 software package [22] on an Origin/3800 server.

3. Results and discussion

3.1. The ground state structural properties

The main optimized geometry structural parameters of **P1**–**P4** and **DP2**–**DP4** are listed in Table 1. As examples, the optimized geometry structures of **P4** and **DP4** are shown in Fig. 2, and the Cartesian coordinates and energies for **P1**–**P4** and **DP2**–**DP4** are available in Supplementary data. For all the oligomers, the calculated dihedral angles of C(1)–C(2)–N(4)–C(8)/C(14)–C(16)–C(17)–C(21)/N(3)–C(1)–C(2)–C(6)/N(4)–C(8)–C(10)–C(12)/C(8)–C(10)–C(14)–C(16)/C(17)–C(21)–C(20)–C(19) are almost 180.0° and/or 0.0°, meaning that BTE units keep the respective geometry as free molecule upon aggregating to the oligomer. Therefore, we can propose that the P-polymer and DP-polymers should be planar due to the following two reasons: (1) the ethynyl and bipyridyl substitutes in oligomers are rigid; (2) the π–π interactions between pyridyl groups tend to significantly reduce the torsion angles between the adjacent units [23,24], the dihedral angles between the adjacent pyridine rings are fixed up by bridge atoms, which tend to keep the planar structures.

The calculated bond angles of C(2)–C(6)–C(12)/C(2)–N(4)–C(8)/C(6)–C(2)–N(4)/C(8)–C(10)–C(12) in all the oligomers are close to 120.0°, which indicates that the geometry structures of the bipyridyl groups are hardly changed with the increase of the chain length. As shown in Fig. 2, all the oligomers display zigzag structures with the angle of 150.0° between the two neighbor repeating units; we think this kind of arrangement can reduce the steric effect and stabilize the molecules at the largest extent.

The bond lengths in the bipyridyl and thiophenyl fragments of **P1**–**P4** and **DP2**–**DP4** do not vary as the conjugated chains

Table 1
The optimized geometry structural parameters of **P1**–**P4** and **DP2**–**DP4** in the ground state (X^1A) under the B3LYP and the excited state (A^1B) under CIS level

	P1 X^1A/A^1B	**P2** X^1A/A^1B	**P3** X^1A	**P4** X^1A	**DP2** X^1A/A^1B	**DP3** X^1A	**DP4** X^1A
Bond length (Å)							
C(1)–C(2)	1.474/1.421	1.474/1.462	1.474	1.474	1.475/1.465	1.474	1.474
C(2)–N(4)	1.360/1.367	1.360/1.345	1.360	1.360	1.36/1.344	1.360	1.36
C(9)–C(13)	1.418/1.396	1.418/1.426	1.418	1.418	1.426/1.430	1.426	1.426
C(10)–C(14)		1.417/1.400	1.417	1.417	1.417/1.400	1.417	1.417
C(22)–C(23)	1.766/1.749	1.766/1.741	1.766	1.766			
C(13)–C(15)	1.223/1.215	1.223/1.200	1.223	1.223	1.215/1.196	1.215	1.215
C(14)–C(16)		1.223/1.219	1.223	1.223	1.223/1.220	1.223	1.223
C(16)–C(17)		1.403/1.376	1.403	1.403	1.403/1.374	1.403	1.403
C(17)–C(18)		1.762/1.758	1.762	1.762	1.762/1.759	1.762	1.762
Bond angle (°)							
C(2)–C(6)–C(12)	119.3/119.7	119.3/119.3	119.3	119.3	119.3/119.3	119.3	119.3
C(2)–N(4)–C(8)	119.2/120.3	119.2/120.5	119.3	119.2	119.2/120.5	119.2	119.2
C(6)–C(2)–N(4)	121.4/120.2	121.4/120.8	121.4	121.5	121.5/120.9	121.5	121.5
C(8)–C(10)–C(12)	117.0/116.8	117.0/116.8	117.0	117.1	117.1/116.8	117.1	117.1
C(10)–C(14)–C(16)	179.8/179.9	180.0/180.0	179.9	179.9	179.9/180.0	179.5	179.4
C(14)–C(16)–C(17)	179.5/180.0	179.8/179.8	179.6	179.4	179.4/179.8	179.8	179.4
Dihedral angle (°)							
C(1)–C(2)–N(4)–C(8)	180.0/180.0	180.0/180.0	180.0	180.0	180.0/180.0	180.0	180.0
C(3)–C(1)–C(2)–C(6)	0.0/−0.0	0.0/0.0	0.01	0.0	−0.0/0.0	0.1	−0.0
C(4)–C(8)–C(10)–C(12)	−0.0/0.0	0.0/0.0	0.0	0.0	0.0/0.0	−0.0	0.0
C(8)–C(10)–C(14)–C(16)	0.2/−0.6	0.0/0.0	0.6	0.4	0.0/2.1	1.0	0.2
C(14)–C(16)–C(17)–C(21)	179.9/174.2	179.9/179.9	179.9	180.0	179.8/179.8	178.0	180.0
C(17)–C(21)–C(20)–C(19)		0.0/0.0	0.0	0.0	0.0/0.0	0.0	0.0

are elongated expecting that the bond lengths of C(9)–C(13) and C(13)–C(15) in ethynyl units change somewhat from **P2**–**P4** to **DP2**–**DP4**. The single bond C(9)–C(13) is 1.418 Å in **P1**–**P4** but 1.426 Å in **DP2**–**DP4**, while the triple bond C(13)–C(15) is 1.223 Å in **P1**–**P4** but 1.215 Å in **DP2**–**DP4**. The bond length variation from the P-oligomer to DP-oligomer is due to the presence of the tail thiophenyl fragments in the P-oligomers which leads to the stronger conjugation effects compared with the DP-oligomers and results in the relaxation of C(13)–C(15) bond and strengthening of C(9)–C(13) bond.

3.2. The properties of the frontier molecular orbitals in the ground state

The molecular orbital compositions of **P1**–**P4** and **DP2**–**DP4** in the ground state are listed in Table 2. We note that both the HOMOs and LUMOs of **P1**–**P4** and **DP2**–**DP4** spread over the whole π-conjugated backbones and have the similar character. As examples, the HOMO and LUMO density diagrams of **P1**, **P4** and **DP4** are shown in Fig. 3. As shown in Fig. 3, the HOMO displays antibonding character between two adjacent fragments and bonding character within ethynyl, bipyridyl and thiophenyl parts. But the LUMOs exhibit the bonding character between the two adjacent fragments. There is a tendency both in HOMO and LUMO for either the P-oligomer or the DP-oligomer to populate the electrons on the central chromophore. Taking **P4** for example, in the HOMO, MO 159a, with π character, the terminal thiophenyl groups take up only 17% of the whole MO, while in the LUMO, MO 156b, with π* character, lying above the HOMO by about 2.7 eV, just has the composition of terminal thiophenyl groups of 11%. This indicates that the oligomers show good π-conjugated effect.

The HOMO and LUMO energies have a trend to converge. We find that the shift of HOMO energy ($\Delta\varepsilon_{HOMO}$) drops from an initial step of 0.122 eV (between **P1** and **P2**) to 0.028 eV (between **P2** and **P3**) and to 0.007 eV (between **P3** and **P4**). The values of $\Delta\varepsilon_{HOMO}$ become smaller with the increase of the chain length and the same variation trend is observed for the LUMO. The LUMO of **P1** is 0.3–0.4 eV higher than that of **P2**, **P3** and **P4**. Analyzing the orbital, the LUMO of **P1** is dominantly contributed from the bipyridine groups with 60% compositions while the LUMOs of **P2**, **P3** and **P4** have a lower composition of the bipyridyl groups (50% compositions) (See Table 2).

Table 2 shows that whether in the P-oligomers or in the corresponding DP-oligomers, the HOMO–LUMO gap is narrowed gradually, which implies that it is easier to promote an electron from the HOMO to the LUMO when the chain length is getting longer. Moreover, the HOMO–LUMO gaps of the P-oligomer are smaller than those of the corresponding DP-oligomers, indicating that the intense π-conjugated interaction can lower the HOMO–LUMO gaps, which is in accordance with the measured red-shifted absorption spectra as the increase of the chain length [10]. Therefore, the electron transition behavior can be adjusted through designing the P-oligomer or DP-oligomers, so that the favorable optical spectra can be obtained.

Fig. 4 shows that there is a good linear relationship between the HOMO–LUMO gaps and the inverse repeating unit numbers $1/n$ for P-oligomers and DP-oligomers. Through the extrapolation method, we obtain the very similar HOMO–LUMO gap of the P-polymer (2.55 eV) and DP-polymer

Table 2
The molecular orbital energies (eV) and compositions (%) of **P1–P4** and **DP2–DP4** in the ground state under the B3LYP calculations

		Energy	Bipyridyl	Ethynyl	Thiophenyl
P1	LUMO + 1 (48b)	−1.3540	19.8	16.2	64.0
	LUMO (49a)	−2.1886	60.3	13.9	25.8
	HOMO (47b)	−5.5438	36.9	25.5	37.6
	HOMO − 1 (48a)	−6.0198	16.8	27.4	55.7
P2	LUMO + 2 (85b)	−1.6014	26.6	17.9	55.5
	LUMO + 1 (86a)	−2.0931	64.4	13.5	22.2
	LUMO (84b)	−2.5059	51.8	17.6	30.6
	HOMO (85a)	−5.4219	36.2	28.8	35.0
	HOMO − 1 (83b)	−5.7531	34.5	25.8	39.6
	HOMO − 2 (84a)	−5.9825	19.2	29.4	51.3
P3	LUMO + 3 (122b)	−1.7045	29.6	18.4	51.9
	LUMO + 2 (123a)	−2.0518	66.7	13.3	20.1
	LUMO + 1(121b)	−2.3704	51.9	17.2	30.9
	LUMO (122a)	−2.6142	51.4	18.2	30.4
	HOMO (120b)	−5.3944	36.2	29.4	34.4
	HOMO − 1 (121a)	−5.5653	35.2	28.6	36.2
	HOMO − 2 (119b)	−5.8402	31.4	26.9	41.7
	HOMO − 3 (120a)	−5.9675	20.2	30.2	49.6
P4	LUMO + 3 (161a)	−2.0303	68.1	13.1	18.8
	LUMO + 2 (157b)	−2.2874	52.1	16.9	30.9
	LUMO + 1(160a)	−2.5037	51.4	17.8	30.8
	LUMO (156b)	−2.6651	51.4	18.3	30.3
	HOMO (159a)	−5.3874	36.3	29.5	34.2
	HOMO + 1 (155b)	−5.4899	35.7	29.1	35.2
	HOMO + 2 (158a)	−5.6693	33.9	28.9	37.2
	HOMO + 3(154b)	−5.8840	28.8	27.8	43.3
DP2	LUMO + 1 (65a)	−1.9932	82.0	13.7	4.4
	LUMO (63b)	−2.5214	53.3	18.6	28.1
	HOMO (64a)	−5.5629	35.8	30.7	33.5
	HOMO − 1 (62b)	−6.3221	68.9	26.9	4.2
DP3	LUMO + 2 (102a)	−1.9788	81.0	13.0	6.0
	LUMO + 1 (100b)	−2.3620	53.3	18.4	28.4
	LUMO (101a)	−2.6363	52.0	18.5	29.5
	HOMO (99b)	−5.4644	36.1	30.2	33.7
	HOMO − 1 (100a)	−5.7068	33.1	31.3	35.6
	HOMO − 2 (98b)	−6.3496	68.2	26.0	5.8
DP4	LUMO + 4 (138b)	−1.6634	49.3	17.5	33.2
	LUMO + 2 (137b)	−2.2689	52.9	18.2	29.0
	LUMO + 1 (138a)	−2.5124	52.1	18.4	29.5
	LUMO (136b)	−2.6809	51.6	18.5	29.9
	HOMO (137a)	−5.4284	36.2	30.0	33.8
	HOMO − 1 (135b)	−5.5789	35.0	30.6	34.4
	HOMO − 2 (136b)	−5.7841	30.5	31.8	37.7

(2.57 eV). The HOMO–LUMO gap of polyfluorene calculated at B3LYP/6-31G level by Wang and Feng [6b] is 2.91 eV, 0.36 eV higher than our systems. So the conjugated systems we studied are easier to promote the electron from HOMO to LUMO than the polyfluorene. Hörhold and Opfermann [25] reported that the band gap of PPV is evaluated at 2.4 eV using different experimental method, and Brédas et al. [26] calculated a theoretical value of 2.5 eV, Okada et al. [27] reported that the H–L gap of neutral polythiophene is 2.1 eV. These reported systems are better electron-transporting materials and have the similar band gap values as ours. So the conjugated systems we studied are suitable for electron transition.

3.3. Ionization potentials and electron affinities

The calculated IPs (v, a), EAs (v, a), HEP and EEP are listed in Table 3. The values of the IPs (v, a) and HEP progressively decrease while the EAs (v, a) and EEP turn high gradually from $n = 1$ to $n = 4$. The values of IPs, EAs and extraction potentials show good linear relationship with $1/n$. Fig. 4 shows that when the chain length is infinitely elongated to $n = \infty$, the vertical and adiabatic energies required to extract an electron from the neutral molecule are 5.54 and 5.57, and 5.44 and 5.49 eV for P-polymer and DP-polymer, respectively, which indicate that DP-polymer is easier to lose an electron than P-polymer. The EA (v/a) energies needed to

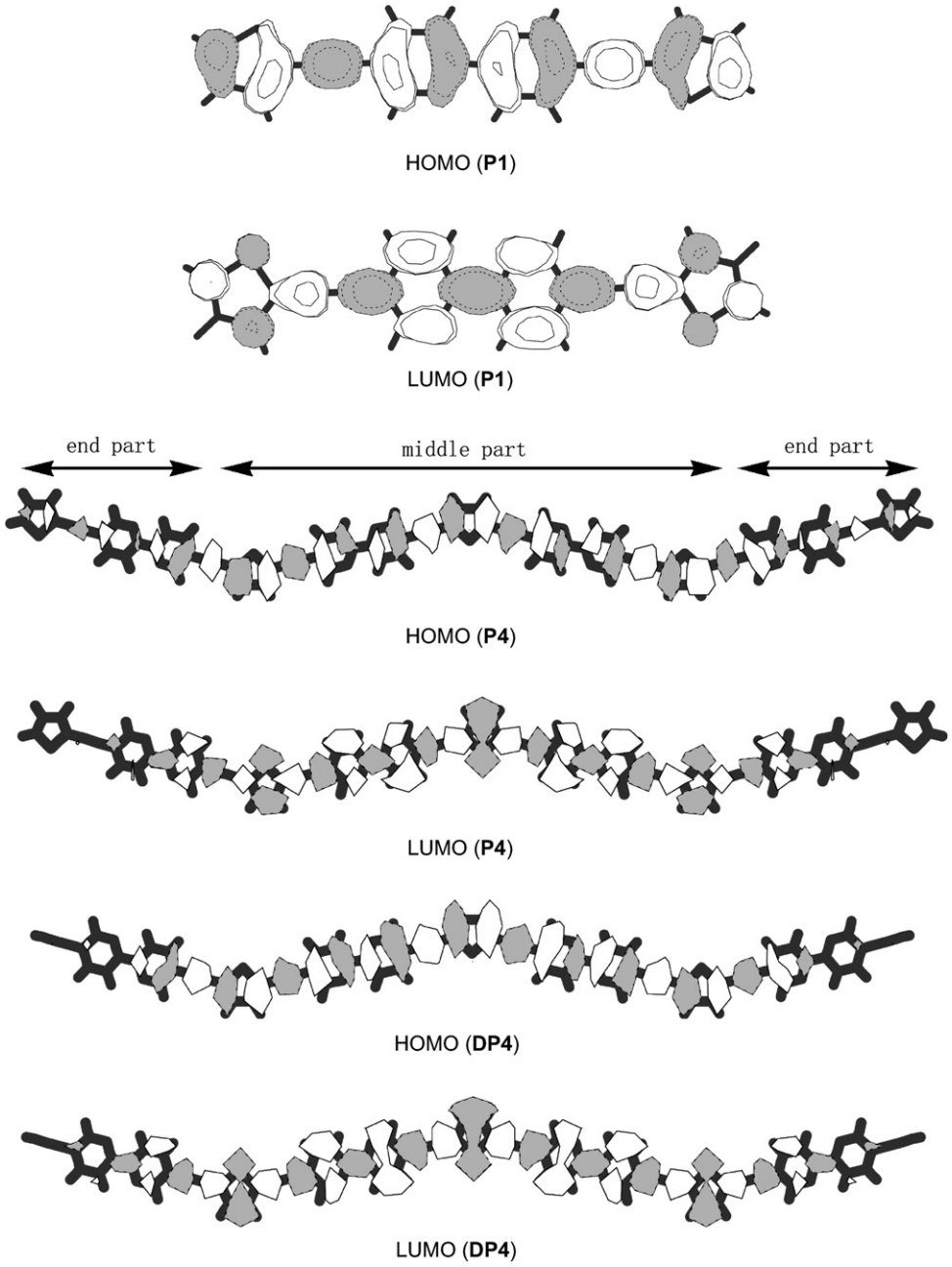

Fig. 3. Electron density diagrams of the HOMO and LUMO for **P1**, **P4** and **DP4**.

create a hole in the polymer are nearly 2.62/2.58 and 2.75/2.63 eV for P-polymer and DP-polymer, respectively, meaning that DP-polymer is apt to create a hole than P-oligomer because of the bigger EA (*v*/*a*) energies. The extraction of a hole from the cation (HEP) needs 5.57 and 5.52 eV and an electron can be extracted from the anion (EEP) with 2.58 and 2.59 eV for P-polymer and DP-polymer, respectively. So DP-polymer is more suitable for electron transferring and hole creating than P-polymer. To appreciate the applicability of our systems we compare the ionization potential and electron affinity to those of polypyridine (PPY) reported experimentally by Miyamae et al. [28]. The IP of PPY (6.3 eV) is 0.37 and 0.86 eV higher than P-polymer and DP-polymer while the EA of PPY (3.5 eV) is higher than P-polymer and DP-polymer by 0.88 and 0.75 eV, respectively. So the electron-donating abilities of DP-polymer are better than P-polymer and PPY.

3.4. Absorption spectra

The calculated dipole-allowed absorptions associated with the oscillator strengths and the assignments are listed in Table 4, the simulated Gaussian type absorption spectra (the half-wave width is 15 nm) are shown in Fig. 5. The simulated spectra appear to be similar in shape with the measured ones [10b] except some red shifts.

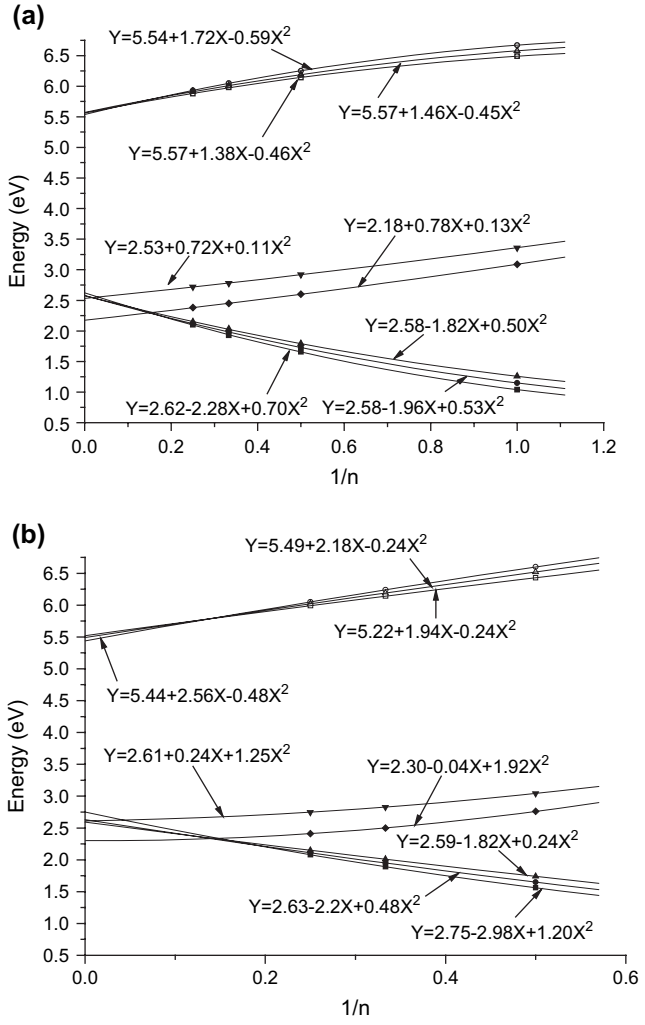

Fig. 4. Δ_{H-L} (□), EA (*v*) (○), EA (*a*) (△), EEP (▼), E_g (◆), IP (*v*) (▲), IP (*a*) (●) and HEP (■) as a function (*Y*) of reciprocal chain length 1/*n* (*X*) for (a) **P1**–**P4** and (b) **DP2**–**DP4** under the B3LYP calculations.

Table 4 shows that the $X^1A \rightarrow A^1B$ absorption at 401, 476, 507, 520 nm and 449, 495, 515 nm for **P1**–**P4** and **DP2**–**DP4**, respectively, are all from the electron promotion from HOMO to LUMO. Take **P1** as example, Table 2 and Fig. 6 show that HOMO (47b) of **P1** is a π type molecular orbitals which are made up of bipyridyl, ethynyl and thiophenyl with the composition of 36.9%, 25.5%, and 37.6%, respectively, while the LUMO (49a) distributes on three fragments with the composition of 60.3%, 13.9%, and 25.8% and displays as the π* type molecular orbital. The frontier orbitals of **P2**–**P4** and **DP2**–**DP4** have the similar character with **P1**. Therefore, the $X^1A \rightarrow A^1B$ transitions for **P1**–**P4** and **DP2**–**DP4** are all assigned to π → π* type transition (see Fig. 6). Furthermore, the calculated $X^1A \rightarrow A^1B$ absorptions are progressively red-shifted from **P1** to **P4** and from **DP2** to **DP4**. Experimentally, Ziessel and co-workers [10] concluded that the lowest-lying absorption shifts progressively toward lower-energy region as the increase of the BTE unit, which is in good agreement with our finding. Both the experimental and the theoretical results indicate that the lowest-lying absorption for the infinite conjugated polymer should tend to a limit since the HOMO–LUMO energy gaps for the polymeric system converges. Here the calculated lower-energy absorptions are underestimated compared to the experimental result (0.3–0.6 eV), this is because the calculation is performed on the isolated gas-phase system, while the experimental absorption spectra are measured in a dichloromethane (1×10^{-5} M) solution [10b], in which the surroundings could perturb the transition to some extent. However, the gradually decreasing lowest-lying absorptions in the order of **P4** < **DP4** < **P3** < **DP3** < **P2** < **DP2** < **P1** on experiment is well reproduced by the TD-DFT calculation results (See Fig. 5). Fig. 5b shows that the lowest-lying absorptions for DP-oligomers are blue-shifted relative to those of the corresponding P-oligomers, which echo the result that the HOMO–LUMO energy gap of the DP-oligomer is higher than that of the P-oligomer. Fig. 4 shows good linear relationship between the lowest-lying absorption and the reciprocal chain length of the oligomers. With the extrapolation method, we obtain the lowest-lying absorption of 2.18 eV for P-polymer which is lower than that of 2.30 eV for DP-polymer, this result is in accordance with the H–L gap regularity.

Table 3
The ionization potentials (eV) and electron affinities (eV) of **P1**–**P4** and **DP2**–**DP4** under the B3LYP calculations

	P1	**P2**	**P3**	**P4**	P-polymer	**DP2**	**DP3**	**DP4**	DP-polymer
IP (*v*)	6.67	6.25	6.05	5.93	5.54	6.60	6.24	6.05	5.44
IP (*a*)	6.58	6.19	6.01	5.91	5.57	6.52	6.19	6.02	5.49
HEP	6.49	6.14	5.98	5.88	5.57	6.43	6.14	5.99	5.52
EA (*v*)	1.04	1.66	1.93	2.10	2.62	1.56	1.89	2.08	2.75
EA (*a*)	1.15	1.73	1.98	2.12	2.58	1.65	1.95	2.11	2.63
EEP	1.26	1.79	2.03	2.15	2.58	1.74	2.01	2.15	2.59

Another differential absorption is at 284, 358, 412, 439 nm, and 293, 393, 427 nm for **P1**–**P4** and **DP2**–**DP4**, respectively, and they have the similar transition character. Table 4 shows that, take **P3** as a prototype, the electron excitation from MO 121a (HOMO − 1) to MO 121b (LUMO + 1) with the CI coefficient of 0.60909 is responsible for the absorption at 412 nm of **P3**. MO 121a and MO 121b of **P3** are π and π* type orbitals (Table 2) with the composition of 35.2%, 28.6%, and 36.2% and 51.9%, 17.2%, and 30.9% for bipyridyl, ethynyl and thiophenyl, respectively, so the absorption at 412 nm for **P3** is originated from the π → π* electron transition.

The other calculated higher energy absorptions are all attributed to the π → π* electron transition.

3.5. The geometry structures in the excited state and the emission

The geometry structure optimization result shows that the oligomers still exhibit planar structures in the A^1B excited state and the geometry structural parameters are very similar as those in the ground state (Table 1). The bond angles in the excited state are slightly changed within 1°. Most of the bond lengths such as C(1)–C(2)/C(9)–C(13)/C(2)–N(4)/

Table 4
The calculated dipole-allowed absorptions for **P1**–**P4** and **DP2**–**DP4** under the TD-B3LYP calculations together with the experimental data

	Transition	Config. (CI coeff)	λ, nm (eV)	Oscillator	Characters	Expt (eV)[10b]
P1	$X^1A \rightarrow A^1B$	47b → 49a (0.65612)	401 (3.09)	2.1139	HOMO → LUMO	3.38
	$X^1A \rightarrow B^1B$	48a → 48b (0.59786)	284 (4.37)	0.3070	HOMO − 1 → LUMO + 1	
P2	$X^1A \rightarrow A^1B$	85a → 84b (0.66099)	476 (2.60)	3.6862	HOMO → LUMO	3.06
	$X^1A \rightarrow B^1B$	83b → 86a (0.63399)	358 (3.46)	0.6665	HOMO − 1 → LUMO + 1	
	$X^1A \rightarrow C^1B$	84a → 85b (0.65288)	298 (4.16)	0.3743	HOMO − 2 → LUMO + 2	
P3	$X^1A \rightarrow A^1B$	120b → 122a (0.65523)	507 (2.45)	5.2742	HOMO → LUMO	3.02
	$X^1A \rightarrow B^1B$	121a → 121b (0.60909)	412 (3.01)	1.0446	HOMO − 1 → LUMO + 1	
	$X^1A \rightarrow C^1B$	119b → 121a (0.64496)	343 (3.62)	0.4999	HOMO − 2 → LUMO + 2	
	$X^1A \rightarrow D^1B$	120a → 120b (0.65588)	304 (4.08)	0.3765	HOMO − 3 → LUMO + 3	
P4	$X^1A \rightarrow A^1B$	159a → 156b (0.63372)	520 (2.38)	6.9334	HOMO → LUMO	2.98
	$X^1A \rightarrow B^1B$	155b → 160a (0.61032)	439 (2.82)	1.2774	HOMO − 1 → LUMO + 1	
	$X^1A \rightarrow C^1B$	158a → 157b (0.59297)	383 (3.23)	0.5950	HOMO − 2 → LUMO + 2	
	$X^1A \rightarrow D^1B$	154b → 161a(0.65116)	334 (3.71)	0.4413	HOMO − 3 → LUMO + 3	
DP2	$X^1A \rightarrow A^1B$	64a → 63b (0.65396)	449 (2.76)	2.7858	HOMO → LUMO	3.14
	$X^1A \rightarrow B^1B$	62b → 65a (0.39240)	293 (4.23)	0.3689	HOMO − 1 → LUMO + 1	
DP3	$X^1A \rightarrow A^1B$	99b → 101a (0.66091)	495 (2.50)	4.4445	HOMO → LUMO	3.02
	$X^1A \rightarrow B^1B$	100a → 100b (0.65924)	393 (3.15)	0.9161	HOMO − 1 → LUMO + 1	
	$X^1A \rightarrow C^1B$	98b → 100a (0.38703)	291 (4.25)	0.2701	HOMO − 2 → LUMO + 2	
DP4	$X^1A \rightarrow A^1B$	137a → 136b (0.64622)	515 (2.41)	6.0788	HOMO → LUMO	2.97
	$X^1A \rightarrow B^1B$	135b → 138a (0.62654)	427 (2.90)	1.0996	HOMO − 1 → LUMO + 1	
	$X^1A \rightarrow C^1B$	136a → 137b (0.66515)	370 (3.35)	0.5629	HOMO − 2 → LUMO + 2	
	$X^1A \rightarrow D^1B$	136a → 138b (0.52082)	318 (3.91)	0.1687	HOMO − 2 → LUMO + 4	

C(13)–C(15) are shortened less than 0.05 Å compared with those in the ground states, so the geometry structures in the excited states become slightly compact. Comparing the geometry structure of **P2** with **DP2** in the A^1B excited state, it shows that the bond lengths of the central fragments hardly changed, while those at terminal fragment varied regularly. From **DP2** to **P2**, the single bond C(9)–C(13) is strengthened (1.430 Å in **DP2**, 1.426 Å in **P2**), while the triplet bond C(13)–C(15) is relaxed (1.196 Å in **DP2**, 1.200 Å in **P2**), the same variation trend has been revealed for the ground state.

The calculated fluorescence of **P1**, **P2** and **DP2** as well as the corresponding experimental data is summarized in Table 5. The calculated fluorescence at 423 nm for **P1** and 490 nm for **P2** shows a red-shifted trend with the elongation of the conjugated chain, which is similar to the case of the absorption. Furthermore the fluorescence of **DP2** at 471 nm is lower in energy than that of **P1** and higher than that of **P2**, manifesting again that the introduction of the unsaturated fragment at the end of the molecule can enhance the conjugation effect and influence the emission. Through analyzing the transition configuration for the fluorescence, we find that the calculated fluorescence is just the reverse process of the calculated absorption $X^1A \rightarrow A^1B$, since both emissions and the lowest-lying absorptions have the same symmetries and transition characters. The Stokes shifts between the calculated lowest-lying absorptions and emissions are 0.159, 0.074 and 0.131 eV for **P1**, **P2**

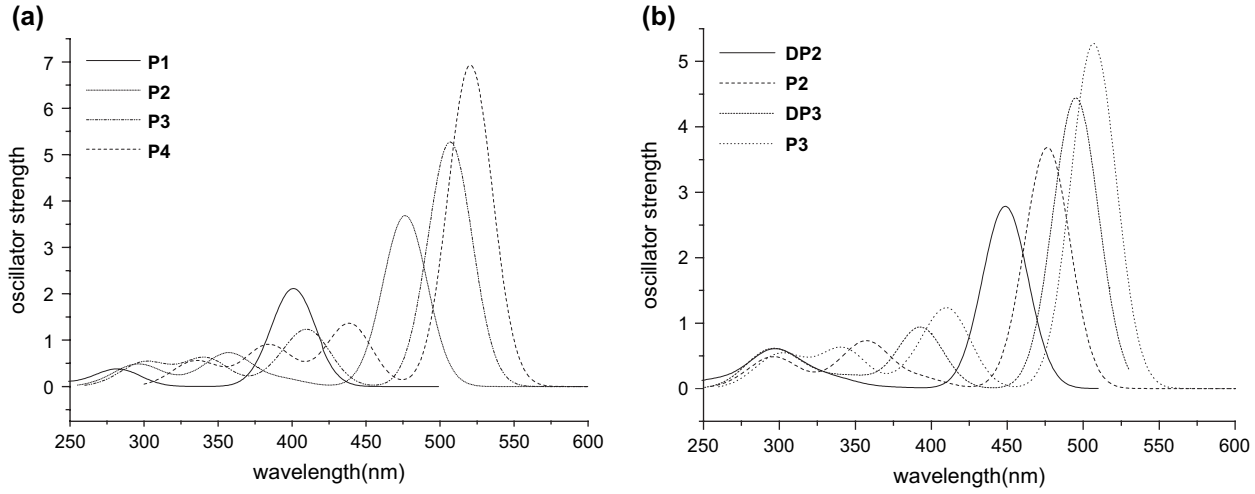

Fig. 5. (a) The fitted Gaussian type absorption spectra for **P1**–**P4**. (b) The fitted Gaussian type absorption spectra for **P2**, **P3**, **DP2**, **DP3**.

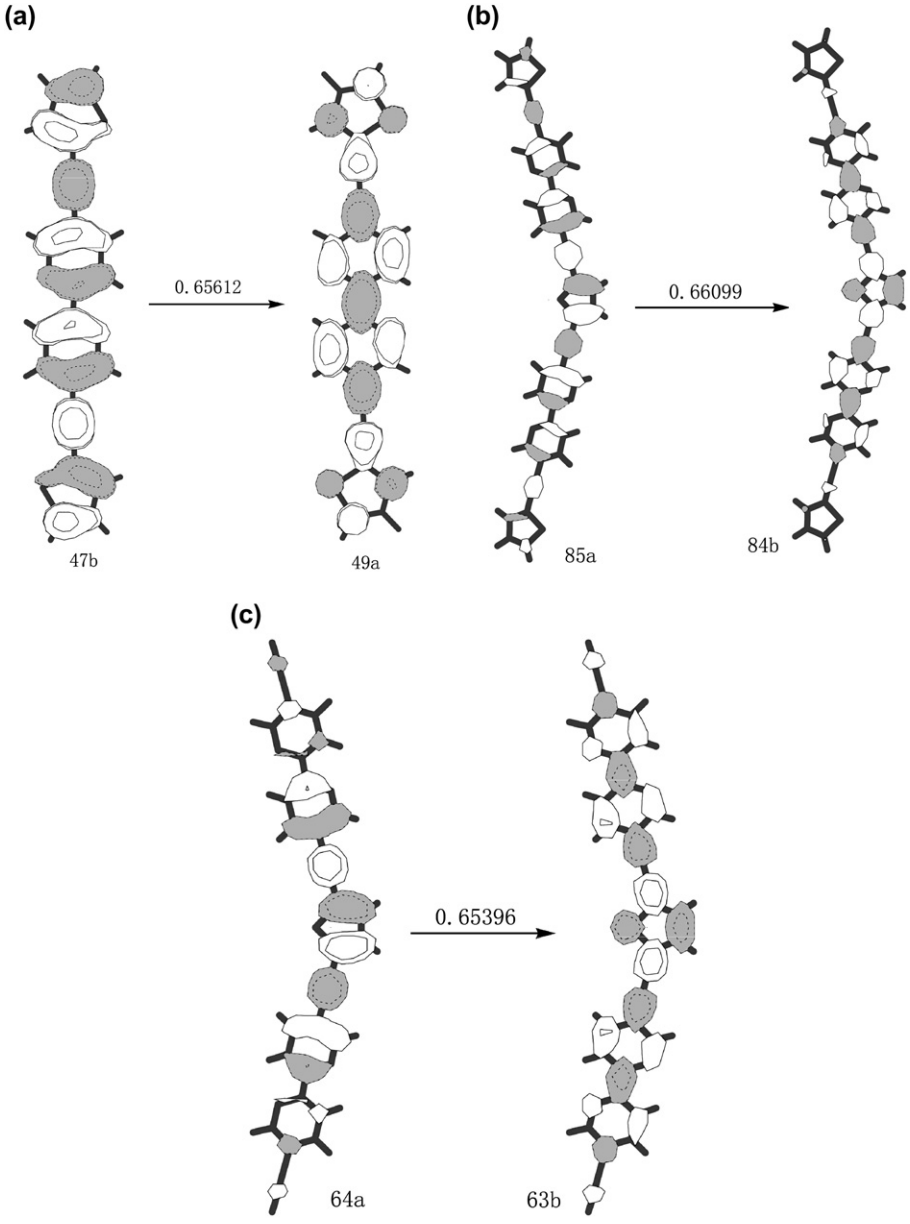

Fig. 6. The density diagram plots of the absorption at 401, 476, and 449 nm for **P1** (a), **P2** (b), and **DP2** (c), respectively, with |CI coefficient| > 0.1 under the TD-B3LYP calculations.

and **DP2**, respectively, and the modest shifts are in agreement with the slight change of the geometry structures from the ground state to the excited state.

There is some deviation between the calculated fluorescence and the experimental result; this is also due to the different environment for the system to stay. The theoretical model is an ideal gas-phase system, while the experimental emission spectra are measured in a dichloromethane (1×10^{-7} M) solution [10b], in which the solution surroundings may influence the emission to some extent. Furthermore, due to the planar geometry structure, the π−π aggregation interactions may exist in the solid state and solvent media which can affect the emission to some extent.

Table 5
The calculated fluorescence emissions of **P1**, **P2** and **DP2** under the TD-B3LYP calculations, together with the experimental data

	Transition	λ (nm)	Config. (CI coeff)	Oscillator	Expt (nm)[10b]
P1	π* → π	423	46b → 50a(0.64369)	2.2985	426
P2	π* → π	490	84b → 85a(0.64853)	3.6962	454
DP2	π* → π	471	63b → 64a (0.64028)	2.8963	449

4. Conclusions

The present work studied the electronic structures, absorption and fluorescence properties of a series of conjugated oligomers involving the bipyridyl, thiophenyl and ethynyl fragments. The oligomers show smooth binomial relationship

between the molecular chain length and the H–L energy gap, IPs, EAs, EEP, HEP, E_g and the optical properties. By extrapolation method, we predict the properties of the P-polymer and DP-polymer. The calculation results indicate that P-polymer and DP-polymer are suitable for hole-transporting and charge transfer materials, moreover DP-polymer is more favorable than the P-polymer. Furthermore, the fluorescence is with some significant shifts between the P-oligomer and DP-oligomer, which is very intriguing for the photosensor or OLED. In a word, the calculation predicts the favorable qualities of the P-polymers and DP-polymers as the functional material.

Acknowledgment

This work is supported by the Natural Science Foundation of China (20173021, 20333050 and 20573042).

Appendix A. Supplementary data

Supplementary data associated with this article can be found in the online version at doi:10.1016/j.polymer.2006.11.029.

References

[1] Zhang X, Cote AP, Matzger AJ. J Am Chem Soc 2005;127:10502.
[2] Jorgensen M, Krebs FC. J Org Chem 2004;69:6688.
[3] (a) Tand CW, Van Slyke SA. Appl Phys Lett 1988;51:913;
(b) Garnier F, Yassar A, Hajlaoui R, Horowitz G, Deloffre D, Servet B, et al. J Am Chem Soc 1993;115:8716.
[4] (a) Babel A, Jenekhe SA. J Phys Chem B 2002;106:6129;
(b) Katz HE, Bao Z. J Phys Chem B 2000;104:671.
[5] Lahti PM, Obrzut J, Karasz FE. Macromolecules 1987;20:2023.
[6] (a) Zhou X, Ren A-M, Feng J-K. Polymer 2004;45:7747;
(b) Wang J-F, Feng J-K. Macromolecules 2004;37:3451;
(c) Yang L, Ren A-M, Feng J-K, Wang J-F. J Org Chem 2005;70:3009;
(d) Liao Y, Feng J-K, Yang L, Ren A-M, Zhang H-X. Organometallics 2005;24:385;
(e) Yang L, Ren A-M, Feng J-K, Liu X-D, Ma Y-G, Zhang H-X. Inorg Chem 2004;43:5961;
(f) Yang L, Ren A-M, Feng J-K, Ma YG, Zhang M, Liu X-D, et al. J Phys Chem A 2004;108:6797.
[7] (a) Burroughes JH, Bradley DDC, Brown AR, Marks RN, Mackay K, Friend RH, et al. Nature 1990;347:539;
(b) Yamaguchi Y, Tanaka T, Kobayashi S, Wakamiya T, Matsubara Y, Yoshida Z-I. J Am Chem Soc 2005;127:9332.
[8] (a) Belletete M, Bwaupre S, Bouchard J, Blondin P, Leclerc M, Durocher G. J Phys Chem B 2000;104:9118;
(b) Miyata Y, Nishinaga T, Komatsu K. J Org Chem 2005;70:1147.
[9] Fabiano E, Sala FD, Cingolani R, Weimer M, Gorling A. J Phys Chem A 2005;109:3078.
[10] (a) De Nicola A, Liu Y, Schanze KS, Ziessel R. Chem Commun 2003;288;
(b) Goeb S, Nicola AD, Ziessel R. J Org Chem 2005;70:1518.
[11] Bryce AB, Charnochk JM, Pattrichk RAD, Lennie AR. J Phys Chem A 2003;107:2516.
[12] Pan QJ, Zhang HX. Eur J Inorg Chem 2003;4202.
[13] Naito K, Sakurai M, Egusa S. J Phys Chem A 1997;101:2350.
[14] (a) Casado J, Pappenfus TM, Mann KR, Ortì E, Viruela PM, Milian B, et al. Chem Phys Chem 2004;5:529;
(b) Milian B, Pou-Amerigo R, Viruela R, Orti E. Chem Phys Lett 2004;391:148.
[15] Stephens PJ, Devlin FJ, Chabalowski FCF, Frisch MJ. J Phys Chem 1994;98:11623.
[16] Novoa JJ, Sosa C. J Phys Chem 1995;99:15837.
[17] Raghavachari K, Pople JA. Int J Quantum Chem 1981;20:1067.
[18] Halls MD, Schlegel HB. Chem Mater 2001;13:2632.
[19] (a) Pan Q-J, Zhang H-X. Organometallics 2004;23:5198;
(b) Zhou X, Zhang H-X, Pan Q-J, Xia B-H, Tang A-C. J Phys Chem A 2005;109:8809.
[20] Foresman JB, Head-Gordon M, Pople JA, Frisch MJ. J Phys Chem 1992;96:135.
[21] Casida ME, Jamorski C, Casida KC, Salahub DR. J Chem Phys 1998;108:4439.
[22] Frisch MJ, Trucks GW, Schlegel HB, Scuseria GE, Robb MA, Cheeseman JR, et al. Gaussian 03, revision C.02. Wallingford, CT: Gaussian, Inc.; 2004.
[23] Puschnig P, Ambrosch-Draxl C. Phys Rev B 1999;60:7891.
[24] Colle R, Curioni A. J Phys Chem A 2000;104:8546.
[25] Hörhold H-H, Opfermann J. Makromol Chem 1970;131:105.
[26] (a) Brédas JL, Chance RR, Baughman RH, Silbey R. J Chem Phys 1982;76:3673;
(b) Brédas JL, Silbey R, Boudreaux DS, Chance RR. J Am Chem Soc 1983;105:6555.
[27] Kozaki M, Yonezawa Y, Igarashi H, Okada K. Synth Met 2003;135–136:107.
[28] (a) Miyamae T, Yoshimura D, Ishii H, Ouchi Y, Seki K, Miyazaki T, et al. J Chem Phys 1995;103:2738;
(b) Miyamae T, Yoshimura D, Ishii H, Ouchi Y, Miyazaki T, Koike T, et al. J Electron Spectrosc Relat Phenom 1996;78:399.